Acetylcholine Receptor Aggregation Parallels the Deposition of a Basal Lamina Proteoglycan during Development of the Neuromuscular Junction

M. JOHN ANDERSON, F. GEORGE KLIER, and KAREN E. TANGUAY
Department of Pharmacology and Therapeutics, The University of Calgary, Calgary, Alberta, Canada T2N 4N1; Department of Embryology, Carnegie Institution of Washington, Baltimore, Maryland 21210; and The Salk Institute, La Jolla, California 92138. Dr. Anderson's and Ms. Tanguay's current address is The University of Calgary; Mr. Klier's current address is La Jolla Cancer Research Foundation, La Jolla, California 92138.

ABSTRACT To determine the time course of synaptic differentiation, we made successive observations on identified, nerve-contacted muscle cells developing in culture. The cultures had either been stained with fluorescent α-bungarotoxin, or were maintained in the presence of a fluorescent monoclonal antibody. These probes are directed at acetylcholine receptors (AChR) and a basal lamina proteoglycan, substances that show nearly congruent surface organizations at the adult neuromuscular junction. In other experiments individual muscle cells developing in culture were selected at different stages of AChR accumulation and examined in the electron microscope after serial sectioning along the entire path of nerve–muscle contact.

The results indicate that the nerve-induced formation of AChR aggregates and adjacent plaques of proteoglycan is closely coupled throughout early stages of synapse formation. Developing junctional accumulations of AChR and proteoglycan appeared and grew progressively, throughout a perineural zone that extended along the muscle surface for several micrometers on either side of the nerve process. Unlike junctional AChR accumulations, which disappeared within a day of denervation, both junctional and extrajunctional proteoglycan deposits were stable in size and morphology.

Junctional proteoglycan deposits appeared to correspond to discrete ultrastructural plaques of basal lamina, which were initially separated by broad expanses of lamina-free muscle surface. The extent of this basal lamina, and a corresponding thickening of the postsynaptic membrane, also increased during the accumulation of AChR and proteoglycan along the path of nerve contact. Presynaptic differentiation of synaptic vesicle clusters became detectable at the developing neuromuscular junction only after the formation of postsynaptic plaques containing both AChR and proteoglycan. It is concluded that motor nerves induce a gradual formation and growth of AChR aggregates and stable basal lamina proteoglycan deposits on the muscle surface during development of the neuromuscular junction.

The neuromuscular junction of vertebrate skeletal muscle provides a remarkable example of localized chemical specialization, both for the muscle fiber and motor neuron. The complementarity of pre- and postsynaptic organization, so conspicuous at the frog neuromuscular junction (9), must depend upon some local exchange of regulatory signals between the two cell types at their site of contact. In fact, during formation of the neuromuscular junction the developing nerve induces a reorganization of the muscle plasma membrane, leading to an aggregation of mobile acetylcholine re-

THE JOURNAL OF CELL BIOLOGY · VOLUME 99 NOVEMBER 1984 1769–1784

ceptors (AChR)[1] adjacent to the site of cell contact and the disappearance of AChR accumulations elsewhere on the cell surface (2, 3). Unfortunately, the molecular mechanisms that regulate this phenomenon remain elusive.

There is, nevertheless, evidence that long-lived substances associated with the adult junctional basal lamina can induce the localized development of "synaptic" vesicle clusters (32) in regenerating nerve and corresponding aggregates of AChR in regenerating muscle cells (12). Furthermore, the junctional basal lamina is known to be differentiated chemically from the surrounding, morphologically indistiguishable muscle basal lamina, in its content of acetylcholinesterase (14, 16, 26), a basal lamina heparan sulfate proteoglycan (HSPG) (4), and an assortment of other antigens (31). It further appears that regenerating motor nerves preferentially seek out these specialized regions of basal lamina on the denervated muscle surface during synapse regeneration (32).

It has recently been found that accumulations of HSPG, reminiscent of that at the neuromuscular junction, also appear on aneural embryonic muscle cells developing in culture. Dense plaques of HSPG likewise occur at developing neuromuscular junctions in cell culture (4). These findings raise two possibilities: (*a*) that growing nerve fibers may also seek out such specialized regions of basal lamina during the embryonic development of the neuromuscular junction, or (*b*) that the junctional basal lamina might be induced de novo by the developing motor neuron, as is the junctional accumulation of AChR (2, 3).

To distinguish between these alternatives, we analyzed the time-dependent changes that occur on the muscle cell surface during the development of the amphibian neuromuscular junction in cell culture. In earlier experiments, we compared the surface organization of AChR and HSPG at sites of nerve-muscle contact (4). In the present study, we examined changes in their surface distributions on identified, living cells during synaptogenesis. This has been achieved through the use of fluorescent derivatives of α-bungarotoxin (αBGT) (1) and a monoclonal antibody specific for HSPG (4). In other experiments, we also analyzed the ultrastructure of serially sectioned nerve–muscle contacts that had been selected at different stages of junctional AChR accumulation.

These observations reveal that innervation precedes a gradual deposition of HSPG in the vicinity of the developing synaptic cleft. The appearance of junctional HSPG closely parallels the corresponding aggregation of AChR in the developing postsynaptic membrane. In fact, junctional accumulations of HSPG and AChR remain nearly congruent throughout these early stages of synapse development (4). However, at these stages of development junctional accumulations of AChR, but not HSPG, are unstable and disappear after denervation.

Ultrastructural analysis of identified muscle cells at different stages of synapse development indicates that HSPG deposition and AChR aggregation are associated with the formation and growth of discrete plaques of basal lamina throughout a perineural zone that extends over the muscle surface for several micrometers away from the site of cell contact. At later stages of synapse development, when presynaptic differentiation becomes detectable by conventional ultrastructural techniques, junctional basal lamina fills much of this perineural zone, and often extends beyond the boundaries of the postsynaptic AChR aggregate. Such observations strongly suggest that the localized chemical specialization of the basal lamina and postsynaptic sarcolemma are both coordinated and induced by the motor neuron. Together, these observations indicate that the mechanisms that bring about synaptic differentiation may be under different forms of regulation during embryonic development and adult regeneration.

[1] *Abbreviations used in this paper:* AChR, acetylcholine receptor; αBGT, α-bungarotoxin; HSPG, heparan sulfate proteoglycan; TRITC, tetramethylrhodamine isothiocyanate.

MATERIALS AND METHODS

Preparation of Cultures: The procedures involved in the preparation of cultures containing myotomal muscle and neural tube cells from embryos of *Xenopus laevis* have already been described in detail (3, 22). Dorsal portions of stage 24–26 (27) embryos were dissected in the presence of 1 mg/ml collagenase (Type 1, Worthington Biochemical Corp., Freehold, NJ) in a modified Holtfreter solution to facilitate the isolation of the myotomal musculature and neural tubes. This solution consisted of 67 mM NaCl, 0.5 mM $CaCl_2$, 1.6 mM KCl, and 8 mM HEPES-NaOH (pH 7.4). Myotomal muscle and neural tubes were further dissociated by exposure for 60 min to 1 mg/ml trypsin and 0.4 mg/ml EDTA (Gibco Laboratories, Grand Island, NY) in calcium-free Holtfreter solution, and then plated onto collagen-coated coverslips in sealed culture chambers (see reference 3). The plating medium consisted of 60% vol/vol HEPES-buffered Dulbecco's medium (Gibco Laboratories) supplemented with 5% vol/vol fetal calf serum or dialyzed horse serum. After 1 d in culture the serum concentration was reduced to ~0 5% vol/vol. Muscle cultures were maintained thereafter for an additional 2–3 d at room temperature (22–24°C) or for 1–3 wk at 10°C. To obtain mixed cultures of nerve and muscle cells, freshly isolated neural tubes were dissociated (see above) with trypsin-EDTA and added to established muscle cultures in low-serum maintenance medium, supplemented with 10 μM *d*-tubocurarine (Sigma Chemical Co., St. Louis, MO).

The dissociated neural tubes consisted either of individual cells with spherical perikarya 10–20 μm in diameter, or small cell clusters. During their first day in culture, neurites emerged from the spherical cells to make contact with adjacent muscle cells. These contacts occurred on all regions of the muscle cell surface with no apparent preference in either location or orientation. In most cases the contacts were of the *en passant* variety, and nerve processes could be seen both approaching and leaving the muscle cells. In this respect the nerve–muscle contacts that form in culture resemble those at the myotomal neuromuscular junction in vivo (23, 35). Under the experimental conditions used in this study, nerve growth continued for 2 or more days, during which as many as 80% of the nerve-contacted muscle cells became functionally innervated by cholinergic neurons (5, 22).

Fluorescent Staining of Acetylcholine Receptors: αBGT was prepared from the crude venom of *Bungarus multicinctus* (Miami Serpentarium, Miami, FL) and conjugated with the fluorescent dye tetramethylrhodamine isothiocyanate (TRITC) (Becton-Dickinson & Co., Paramus, NJ) as described previously (1), except for the use of 200 μg of dye per mg of αBGT. The singly labeled dye–toxin derivative was isolated using ion-exchange chromatography (30) and stored at 0.1–0.2 mg/ml (−70°C) for periods up to a year without noticeable loss of potency. Solutions of dye-labeled toxin (10 μg/ml), which were to be used for staining cultured muscle cells, were prepared in culture medium (see above) containing 1% vol/vol dialyzed horse serum or 1% vol/vol fetal bovine serum (Gibco Laboratories) and sterilized by filtration through 0.2-μm pore Fluoropore (Millipore Corp., Medford, MA) membranes. Cultures were stained by exposure to the dye-labeled toxin for 45 min at room temperature (22–24°C) and were then rinsed in the low-serum maintenance medium. When muscle cultures were stained immediately before the addition of neural tube cells, these rinses resulted in at least a million-fold dilution of the labeled toxin over a 20-min period.

Fluorescent Staining of Basal Lamina HSPG: The organization of basal lamina proteoglycan on the myotomal muscle cell surface was revealed by staining with specific monoclonal mouse IgG (2AC2), which had been labeled directly with TRITC. Details of the procedures used to prepare dye-conjugated antibody, and evidence regarding antibody specificity, have been presented earlier (4).

To examine changes in HSPG organization on individual, identified muscle cells after nerve contact, nerve-free muscle cultures were exposed to sterile 10 μg/ml TRITC-labeled antibody for ~1 h at 22–24°C in plating medium (see above), rinsed, and replaced in low-serum maintenance medium (see above) supplemented with ~100 ng/ml of the labeled antibody. This precaution

ensured that recently synthesized HSPG would continuously become stained with the antibody upon its exposure at the cell surface. Dissociated neural tube cells were then added (see above), and the medium was supplemented with 10 μM *d*-tubocurarine to prevent innervated muscle cells from contracting, and thus detaching from the culture dish. Observations were then made in fluorescence and phase-contrast optics, 1 d after adding neural tissue, and on subsequent days at ~24-h intervals. Observation ceased either upon the loss of the muscle cell, usually due to lysis or detachment from the substratum, or when fading of the stain precluded photomicrography. Individual cells were relocated on the basis of their microscope stage coordinates and sketches of the surrounding cells.

Fluorescence Microscopy: The distribution of the TRITC-conjugated αBGT or TRITC-labeled monoclonal antibody (2AC2) bound to the cultured muscle cells was determined with a Zeiss WL microscope (Carl Zeiss, Inc., New York) equipped with a 2FL epicondensor. Light from a high-intensity mercury lamp (HBO 100/W2) was directed onto the culture through two BP546 interference filters, and the resulting fluorescence was examined through either a Zeiss LP580 or a Kodak 23A barrier filter (Eastman Kodak Co., Rochester, NY). Planapochromat Zeiss objectives with magnifications of 63 and 100 were used because of their high numerical apertures (1.4 and 1.3, respectively). With this system it was possible to examine each microscope field using fluorescence and phase-contrast optics. Fluorescence and phase-contrast images of each field were recorded on Ilford HP5 film (Ilford Ltd., Essex, England), which was later processed for 18 min at 20°C in Ilford Microphen developer. Normal exposure times for fluorescence micrographs with the 63× and 100× objectives were 20 and 30 s, respectively.

In negatives of fluorescence micrographs, sites of high AChR or HSPG density appeared as discrete peaks of high grain density. To determine the cumulative area of clustered AChR at the various forms of AChR accumulation at sites of nerve-muscle contact (Fig. 1), measurements were made of apparent AChR cluster areas from 50 examples of each form of AChR accumulation in enlarged photomicrograph negatives. Areas were calculated assuming that each AChR cluster was equivalent to an ellipse with similar axial dimensions. The areas of compound AChR aggregates (Fig. 1) were determined by adding the areas of the individual AChR aggregates present along a single 3–5-μm length of nerve–muscle contact. In each case the fluorescence micrographs had been prepared under similar optical and photographic conditions (see above).

To record the staining at individual nerve–muscle contacts in a single photographic exposure, it was necessary to select examples where the path of the nerve was restricted to the flat surface of the muscle cell facing the collagen-coated substrate. This was of some importance because irradiation of the stained muscle cells with the intense illumination required for fluorescence microscopy caused a progressive fading of the fluorescent image, probably due to bleaching of the fluorescent dye (6).

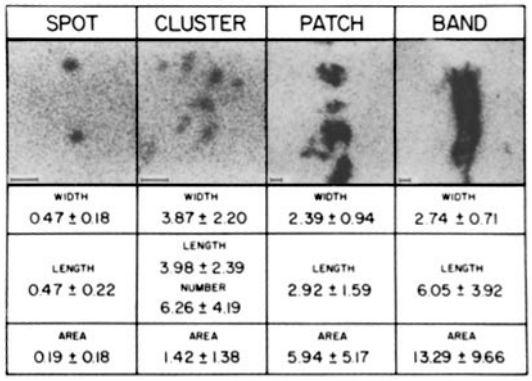

FIGURE 1 Different forms of AChR accumulation at sites of nerve-muscle contact, as visualized by staining with TRITC-labeled αBGT. Negative images of fluorescent micrographs have been greatly enlarged to show details of individual AChR aggregates, and estimates of their dimensions. Patches have been defined as single AChR aggregates >1 μm (see bars in each micrograph) in diameter. AChR "bands" were characterized by particularly intense staining at their borders, and often extended for considerable lengths along the nerve fiber (not shown, but running vertically). Outer dimensions of 50 examples of each AChR accumulation were measured and used to calculate the cumulative area of aggregated AChR, assumed in each case to be approximately equal to an ellipse with similar axial dimensions. The areas of AChR "clusters" were calculated from the number and areas of their constituent AChR "spots." Values are given, together with standard deviations, in micrometers. Note that the obvious differences in morphology of these AChR aggregates also correspond to significant difference in cumulative area.

In experiments that compared the changes in the pattern of staining at separate sites along individual paths of nerve–muscle contact, negative images of the two sequential fluorescence micrographs obtained from individual cells were enlarged and superimposed. Marked changes in the length of the stained region occurred along some paths of nerve contact, usually due to the growth and fusion of adjacent aggregates of AChR or HSPG. Local changes in AChR distribution (refer to Table II) were compiled for each 3–5-μm segment of the nerve contact that showed AChR accumulation at either period of observation. The particularly long regions of clustered AChR that developed on some cells were divided into separate 3–5-μm segments for purposes of analysis.

Denervation of Nerve-contacted Muscle Cells in Culture: To examine the effect of nerve degeneration on AChR distribution, nerve processes leading to some sites of nerve–muscle contact were severed mechanically. In these experiments muscle cultures were stained with TRITC-αBGT immediately before plating neural tube cells (see above), and were maintained thereafter in 10 μM *d*-tubocurarine to prevent muscle contraction. 1 d later we selected muscle cells that had at least one patch or band (see Fig. 1) of intense fluorescent stain along the path of nerve contact. After photographically recording the path of the nerve and the pattern of fluorescent staining, the position of each field was marked and the culture was transferred to the stage of an inverted Zeiss microscope where the previously selected cells were relocated (see above). The culture chamber (3) was partially disassembled, and all nerve processes leading to the selected cells were severed with the tip of a sterile glass microelectrode in regions where the nerve could be seen coursing over the collagen-coated substrate. The culture chamber was then reassembled and filled with the original medium. On the following day, 16–18 h later, the cultures were rinsed in drug-free medium and reexposed to the fluorescent toxin (see above) to ensure that essentially all AChR on the cell surface would be labeled. The previously selected fields were then relocated and the pattern of fluorescent staining was again recorded.

In other experiments the same procedure was followed, except that taipoxin (a gift from Dr. J. Patrick, Salk Institute), a presynaptic toxin from the venom of *Oxyuranus scutatus*, was added to the culture medium (final concentration 5 ng/ml) after selecting nerve-contacted cells and recording the pattern of the fluorescent stain. When placed in cultures of nerve and muscle cells, taipoxin caused the retraction or degeneration of virtually every neurite, thus leading to the denervation of all nerve-contacted cells.

Electron Microscopy: Cultures in which nerve-contacted muscle cells had been stained with TRITC-αBGT and selected for electron microscopy were fixed by exposure for 30 min at 22–24°C to a 1% wt/vol solution of glutaraldehyde (Electron Microscopy Sciences, Ft. Washington, PA) in calcium-free Holtfreter solution (see above), supplemented with 10 mM $MgCl_2$ and 4% vol/vol dimethylsulfoxide. The addition of dimethylsulfoxide to the fixative markedly reduced the swelling and rupture of cytoplasmic organelles that otherwise occurred when myotomal muscle cells were exposed to glutaraldehyde. After extensive rinsing in the high-magnesium Holtfreter solution (see above) the cultures were postfixed for 30 min at room temperature with 2% wt/vol osmium tetroxide in the same buffer, dehydrated in ethanol, and embedded in Epon 812. During dehydration the cells were stained en bloc for 30 min with 4% wt/vol uranyl acetate in 70% vol/vol ethanol.

After the embedding medium had cured, the glass coverslip, which provided the substrate of the culture chamber, was removed by alternately immersing the chamber in liquid nitrogen and warm water. The previously selected fields in the embedded culture were then relocated using phase-contrast optics (see above). Individual fields were marked and cut from the embedded culture using a dental drill. With the aid of a stereomicroscope it was possible to orient each block such that thin sections were cut approximately perpendicular to the path of nerve–muscle contact. Sections were obtained through the fields of interest using a Reichart OMU3 ultramicrotome. These were stained for 5 min with lead citrate and examined in a Hitachi HS-8 electron microscope.

When the organization of the developing junctions was to be determined at different sites along the path of individual nerve–muscle contacts, a different procedure was followed. In these cases the sections (~100 nm thick) from each 20 serial passes of the ultramicrotome knife were maintained as a cluster, and were then mounted together on a single microscope grid. The grids were numbered and examined sequentially. In each of the recovered sections (sections were lost during sectioning and mounting, or became obscured by grid bars) the site of contact between the nerve fascicle and the muscle cells was located, and the presence or absence of synaptic organelles was recorded. The identified organelles included (*a*) synaptic vesicles, (*b*) clusters of five or more

synaptic vesicles within a single nerve fiber, (*c*) "presynaptic densities" associated with the neurilemma, (*d*) accumulation of basal lamina material between the muscle cell and any adjacent nerve fibers, and (*e*) localized, dense staining of the sarcolemma (postsynaptic densities). The organization along each nerve–muscle contact was then reconstructed by plotting the fraction of recovered sections (per grid) containing each synaptic feature as a function of grid number (see Fig. 7).

Contribution of ACh Receptor Turnover to Changes in the Distribution of the Fluorescent Stain: In the present experiments we examined time-dependent changes in the distribution of fluorescent αBGT bound to AChR on cultured muscle cells. In other studies of cultured embryonic muscle (29) ^{125}I-labeled αBGT has been used to demonstrate the internalization and eventual degradation of toxin-receptor complexes. The question thus arose whether the internalization and degradation of toxin-receptor complexes might have contributed to some of the changes in the distribution of the fluorescent stain that were observed in these experiments. It was possible, for example, that some of the observed changes in AChR staining could have reflected localized losses of labeled AChR from the cell surface due either to turnover or the replacement of labeled AChR with newly synthesized AChR. In order to test this possibility 68 of the cells from Table I were reexposed to the fluorescent toxin (see above) immediately after recording the distribution of the stain on the second day after the addition of nerve cells to the cultures. This treatment allowed visualization of AChR which were inserted into the membrane over the 2-d interval after the initial staining.

In all 68 cases, there was a general increase in the intensity of the stain on the muscle cells, but the patterns of stain along individual paths of nerve contact in 59 cases were not significantly different from those in the previous observation made 1 h earlier. When differences in staining could be detected, they involved the shrinkage or disappearance of a few small fluorescent patches or spots (Fig. 1) adjacent to the nerve. These differences were not sufficient on any cell to lead to a change in stage, by the criteria in Fig. 2, and were not seen when other cultures were restained with fluorescein-labeled toxin, and the contrasting fluorochromes examined simultaneously (data not shown). Such minor changes must therefore reflect rearrangements of AChR in the sarcolemma that took place during the period required for restaining. It is thus reasonable to conclude that the changes in the pattern of fluorescent staining presented in Tables I and II actually reflect changes in the distribution of the entire receptor population on the cell surface. The shrinkage or disappearance of stained regions, observed at some sites of nerve–muscle contact, is thus likely to reflect decreases in the size of AChR aggregates.

Although AChR biosynthesis and turnover did not contribute significantly to the changes in the pattern of AChR staining shown in Tables I and II, they may in some cases have led to the appearance of an additional, different form of staining, which was not seen immediately after an initial exposure of the cells to the toxin conjugate. Observations made 2 or more days after staining some cultures with dye-labeled αBGT sometimes revealed a stippling of the stain throughout the entire cell. The amount of stippling was variable between cultures and even among individual cells on the same dish, but occurred on all cells independently of nerve contact. When these small (usually <1 μm) spots of stain were viewed at high magnification, they could be seen to extend throughout the cytoplasm of the muscle cell and appeared in some cases to be associated with equally small phase-dark granules. However, dye associated with these cytoplasmic granules appeared not to be bound to cellular membranes and disappeared after a 15-s fixation at −20°C in ethanol, a treatment that does not affect the distribution of stain associated with AChR on the cell surface (data not shown). These observations suggest that some dye-labeled AChR on the muscle cells became internalized and degraded within cytoplasmic vacuoles, as was previously shown to occur with ^{125}I-labeled αBGT (29).

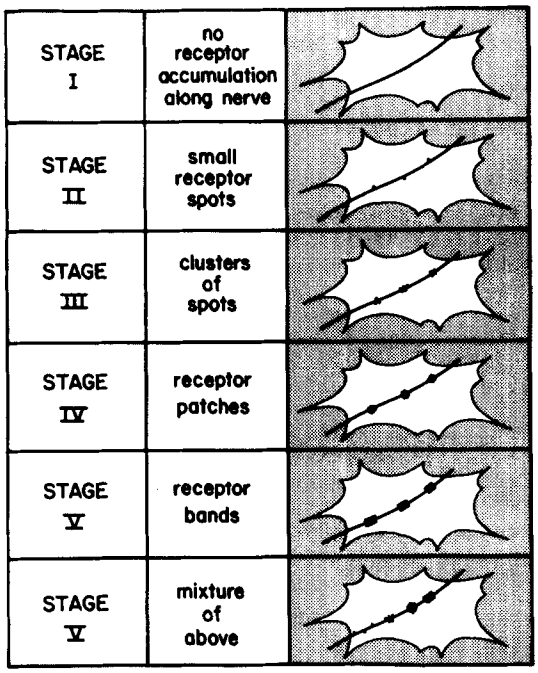

FIGURE 2 Stages of AChR accumulation on different nerve contacted muscle cells. The different forms of AChR aggregate shown in Fig. 1 have been used to define a series of "stages" of increasing AChR accumulation along paths of nerve–muscle contact. When more than one form of AChR aggregate was present, stage was assigned according to the largest and most organized site of AChR accumulation (*bottom panel*). Such classification permits comparisons to be drawn between changes in AChR organization on different muscle cells (see below). Because each of these AChR accumulations is associated with a virtually congruent plaque of HSPG (4), a similar form of classification has also been used to describe changes in the level of HSPG deposition (see below).

RESULTS

In this study we have examined the time courses of two apparently coupled changes in muscle surface organization that take place during synapse formation in cell culture. These dynamic changes have also been compared with detailed ultrastructural observations of selected, stained cells at different stages of synapse development. In earlier studies of this preparation (5, 22), it was shown that progressive increases in the level of spontaneous synaptic activity, reflected in the mean amplitude and frequency of miniature end-plate potentials also parallel changes in the organization of junctional AChR aggregates.

Stages of Postsynaptic Differentiation

To analyze time-dependent changes in muscle surface organization in any detail, it is necessary to introduce descriptive terms that allow distinctions to be drawn between different levels of postsynaptic differentiation (see reference 22). It is already well known that the adult amphibian neuromuscular junction consists of linear arrays of repeating functional units, or "active zones" (15), associated with adjacent invaginations of the postsynaptic membrane. The myotomal neuromuscular junction of *Xenopus laevis* is likely to have a similar modular organization, but does not possess conspicuous junctional folds (13, 23, 35). During synapse development, both the number and maturity of these active zones would be expected to increase at adjacent sites along the path of nerve–muscle contact. However, the absolute number of active zones at different neuromuscular junctions is variable, and continues to change throughout adult life, presumably contributing to matching between the size of the end-plate current and the muscle input impedance (7, 28). Synaptogenesis is thus most appropriately viewed as the development of the initial, differentiated active zones, soon after the establishment of nerve–muscle contact.

When cultured *Xenopus* muscle cells are examined after staining with fluorescent derivatives of αBGT, several forms of AChR accumulation can be distinguished in the vicinity of the nerve fiber at developing neuromuscular junctions (5, 22). These AChR aggregates are associated with congruent deposits of a basal lamina HSPG (4), and can be divided into four morphologically distinguishable forms (see Fig. 1). When

substantial numbers of such AChR accumulations were examined morphometrically (see Materials and Methods), it became clear that the obvious morphological differences (Fig. 1) reflect quantitative differences in the cumulative area of aggregated AChR in the vicinity of the nerve process. It will also be shown (see below) that these sites reflect localized regions of synaptic differentiation. In describing changes that have been observed on individual muscle cells, the "stage" of synaptic development has therefore been assigned on the basis of the largest and most organized (Fig. 1) region of postsynaptic AChR accumulation (see Fig. 2).[2]

Changes in the Organization of AChR Aggregates on Individual Cells

To characterize the time course of nerve-induced changes in AChR organization, we have made successive observations on a group of nerve-contacted muscle cells in cultures that had been briefly exposed to TRITC-labeled αBGT immediately before adding dissociated neural tube cells. It has previously been shown that the AChR distribution on cultured myotomal muscle cells can be recorded photographically for up to 3 d after a single exposure to TRITC-αBGT (2). In the present study we obtained sequential observations of individual nerve-contacted muscle cells on the 1st and 2nd d after adding dissociated neural tube cells to freshly stained myotomal muscle cultures.[3] In the course of these experiments, observations were made over a period of 16–20 h on a total of 192 nerve-contacted muscle cells in 23 cultures. The pattern of AChR staining was recorded photographically at each observation in 103 of these examples. An additional six muscle cells could not be relocated for the second observation and had presumably retracted from the substratum.

The most immediate observation to come out of these experiments was a marked difference in the stability of the path of nerve–muscle contact relative to the pattern of AChR organization. Out of the 192 muscle cells we examined, 164 still had visible nerve contacts in approximately the same position on the following day. A few cells also developed additional sites of nerve contact, either by further growth and branching of the original nerve process, or by the arrival of new nerve fibers. In only 14% of the cells, where the nerve process disappeared entirely, were there noticeable changes in the path of the original nerve. In contrast to this static neuritic morphology, changes in the distribution of labeled AChR occurred along the original nerve, or along newly established paths of nerve contact, on 80% of the cells in this sample by the criteria presented in Fig. 2. In fact, more detailed analysis of the changes at each of the separate sites of AChR accumulation along these nerve contacts (see below) indicated that changes in AChR distribution along the nerve were still more common. However, the net amount of change between observations varied considerably, both between cells and at the separate AChR foci along individual nerve contacts (see Fig. 3). The results of these experiments have thus been analyzed in two ways. We first consider the changes that occurred in AChR organization in the population of cells that were classified according to the criteria presented in Fig. 2. We then examine the changes that occurred at separate foci (Fig. 1) along the path of the nerve on some of those cells where AChR organization was recorded photographically at each observation. Results from the entire group of 192 cells are presented in Table I.

One conspicuous conclusion from the results in Table I is that the net rate of change in AChR distribution, over approximately the same period of time, varied considerably on individual muscle cells. The amount of change at separate foci on individual cells was also variable (see Fig. 3). In spite of such differences between cells, there was a general tendency for the level of AChR organization along the paths of nerve–muscle contact to increase. Altogether, 52% of the cells which retained nerve contact increased one or more stages by the standards used in Fig. 2. This change was quite striking in many cases (Fig. 3) and led to the development of larger AChR patches and bands along the path of the nerve.

It should also be noted, however, that a large proportion of the nerve contacts in this sample (81%) were already associated with discrete AChR accumulations at the time of the initial observation. It remains unclear in such cases whether accumulation of AChR along the path of the nerve could account for the entire AChR aggregate, in that some growing

TABLE I

Cumulative Data

A. Changes in ACh receptor organization on identified muscle cells when nerve contact remained intact

Initial stage	Number of cells	Percentage on day 2 (stage)				
		I	II	III	IV	V
	n			%		
I	36	55	3	0	25	17
II	57	25	9	16	30	21
III	36	11	8	17	42	22
IV	26	8	23	4	30	35
V	10	10	10	0	10	70

B. Changes in ACh receptor distribution when the nerve disappeared

Stage	Initial number	Number of cells on day 2 (stage)				
		I	II	III	IV	V
I	4	4	0	0	0	0
II	5	3	1	1	0	0
III	12	10	1	0	1	0
IV	6	5	0	1	0	0

Cumulative data from 192 identified, nerve-contacted muscle cells, such as those in Figs. 3 and 4, indicating the changes in AChR organization that occurred over the 16–20-h interval between observations. The population of cells was divided into separate groups where the path of nerve–muscle contact appeared to have remained intact (*A*), and where the original nerve fiber could no longer be visualized in phase-contrast optics (*B*). Note that the net change in AChR organization varied greatly on different muscle cells. Nevertheless, the cells tended to increase in stage (*large print*), when the nerve contact survived. Note also the decline in AChR organization (*fine print*) when the nerve contact disappeared between observations.

[2] A small, but highly differentiated, synaptic region thus renders the muscle cell more "mature" than would an extensive contact with minimal synaptic AChR specialization. In fact, even the structurally mature junctions examined in this study had regions of nerve–muscle contact devoid of synaptic specialization (see below).

[3] Because the intensity of the fluorescent stain faded progressively with time, particularly after repeated exposure to the intense illumination required for the preparation of fluorescence micrographs, it was usually practical to record only two successive observations in each field. In order for the staining along the entire length of nerve contact to be recorded in a single photographic exposure, it was also necessary to select examples where nerve fibers had burrowed underneath muscle cells and thus remained associated with the flat surface of the culture dish.

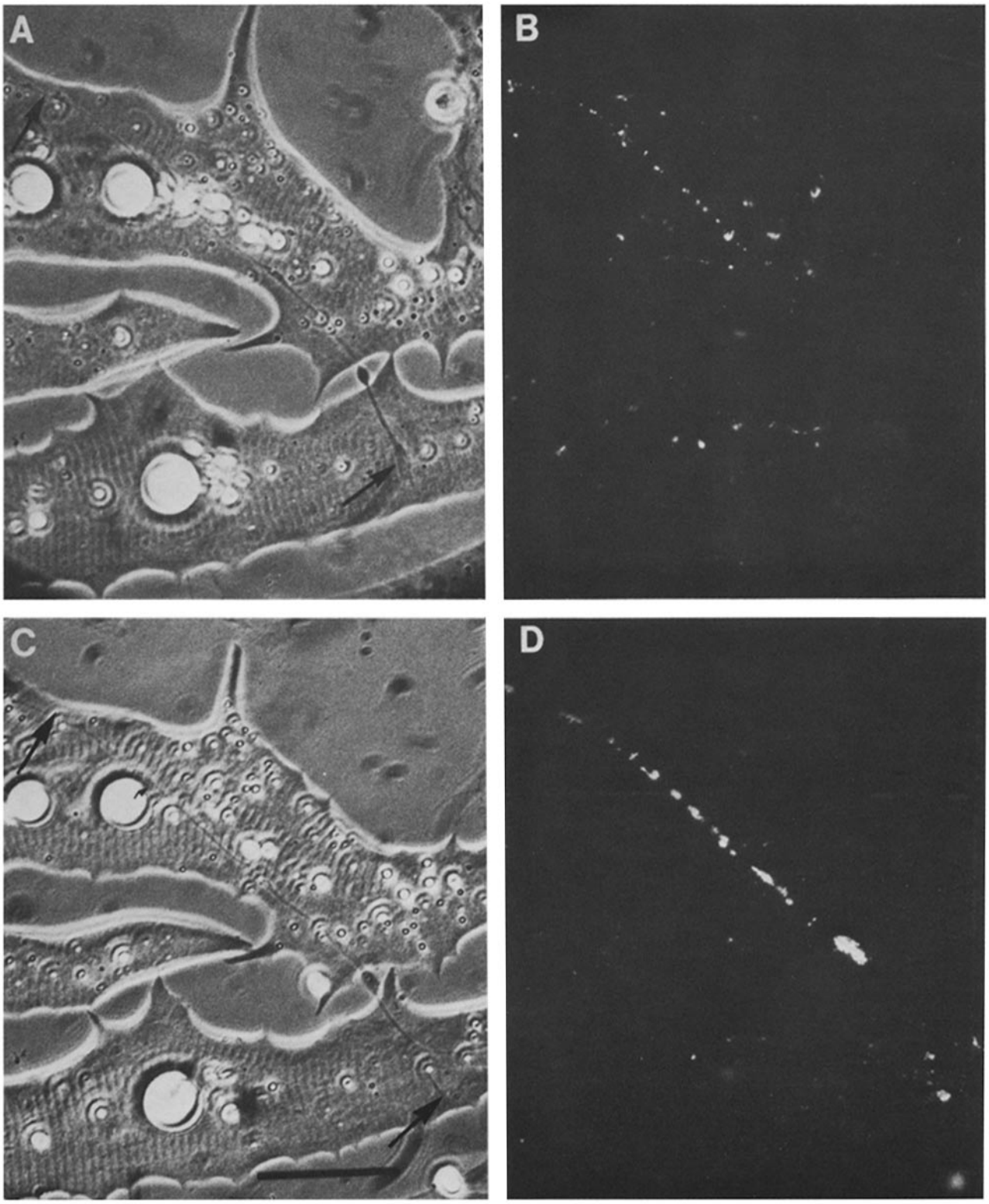

FIGURE 3 Changes in AChR organization (*B* and *D*) on individual nerve-contacted (see arrows in *A* and *C*) muscle cells, between 1 and 2 d after adding dissociated neural tube cells to muscle cultures which had been pulse-labeled with TRITC-αBGT. Note the appearance of new AChR patches (Fig. 1) on the lower cell, which initially had no AChR accumulation near the eventual path of the nerve (stages I–IV, in Fig. 2). Note also the considerable difference between the changes in area of AChR accumulation at adjacent sites of nerve-contact on the upper muscle cell (stages IV–V, in Fig. 2). Bar, 40 μm. × 625.

nerves may initially have become associated with AChR patches which were already present on the muscle cells before their arrival. It is thus also important to consider the fate of those muscle cells that initially had no detectable receptor accumulation at the site of innervation (stage I, Fig. 2). As shown in Fig. 3, some of these cells had only recently become contacted by growing neurites. On about half of these cells (Table I), new AChR accumulations eventually developed

along the recently formed paths of nerve–muscle contact. Even when AChR patches were initially present in the vicinity of the developing nerve fibers, they did not appear to become associated with the eventual path of nerve contact (data not shown). These observations confirm the earlier conclusion that the development of a high AChR density at the site of innervation in this preparation is not dependent upon association of the nerve with the conspicuous AChR patches that were present before nerve–muscle contact (2, 3).

The observations in Table I indicate that some muscle cells with little or no AChR accumulation along the path of the nerve (stages I–III, Fig. 2) later developed larger patches or bands (Fig. 1) along previously established paths of nerve contact. Furthermore, those cells which already had extensive AChR accumulations (stages IV–V, Fig. 2) at the first observation tended to retain them on the following day (Fig. 3). Indeed, the likelihood of an individual muscle cell having at least one large AChR accumulation on the 2nd d after plating nerve cells increased with the stage (Fig. 2) of AChR accumulation during the initial observation (refer to Table I). This result would be expected if nerve-contacted cells were undergoing progressive increases in AChR organization from stages I–V (Fig. 2). In this interpretation, smaller AChR accumulations (Fig. 1) simply represent intermediate forms of receptor organization produced during a gradual formation and growth of AChR aggregates along the path of nerve-muscle contact.

However, a progressive nerve-induced AChR accumulation obviously cannot explain the significant number of examples (18% in Table I), where AChR organization along the path of nerve–muscle contact actually decreased by the criteria in Fig. 2. In fact, no AChR localization was detectable anywhere along the nerve in 20% of those cells that had AChR aggregates on the previous day (see Fig. 4). This was not simply a replacement of labeled AChR due to turnover, because reexposure of the cultures to the stain never revealed additional sites composed primarily of recently synthesized AChR (see Materials and Methods). This observation thus indicates that AChR aggregates along the nerve fiber are not positionally stable at these early stages of development, and remain dependent upon some ongoing action of the muscle cell for their maintenance (10, 33). Likewise, localized differences in the rate of insertion of newly synthesized AChR, or the degradation of surface AChR, do not lead to detectable differences in the organization of AChR in the sarcolemma.

Further understanding of this decrease in AChR aggregation was obtained from cells where the original nerve contact disappeared between the two periods of observation (Table I). In these examples AChR accumulations along the nerve either decreased substantially in size or disappeared entirely. It was thus possible that retraction of part of the nerve fasicle from other muscle cells (see Fig. 4) may have led to a decline in the level of AChR organization. Additional experimental support for this alternative was provided by the observation that denervation of the nerve-contacted cells, 1 d after plating neural tube cells (see Materials and Methods), also led to the disappearance of nerve-associated AChR clusters by the next day (data not shown).

Changes in Receptor Organization at Separate Foci along Paths of Nerve Contact

The results presented in Table I as well as in Figs. 3 and 4 indicate that AChR organization can both increase and decrease at identified nerve–muscle contacts in this preparation. By the criteria used in Fig. 2, there appeared to be an increasing AChR organization at most sites of innervation. However, this system of classification (Fig. 2) deliberately ignores the variation that commonly occurs in AChR organization at adjacent sites on a single muscle cell (see Fig. 3). Therefore, we also analyzed the changes in AChR organization that occurred at each of the separate sites of AChR accumulation along the path of nerve–muscle contact. This was carried out by comparing magnified, superimposed negative images of fluorescence micrographs (see Materials and Methods) to determine the changes in organization that took place at separate foci along each nerve contact. It was of most interest to analyze the changes in AChR organization on those muscle cells that at some time developed at least one extensive AChR accumulation along the path of nerve contact (stages IV–V, Fig. 2). Fluorescence micrographs were obtained from a total of 62 such cells in the course of the experiments presented in Table I. The cumulative data from the 720 separate foci on these cells are presented in Table II.

The data in Table II confirm that AChR organization underwent obvious changes at the majority of the foci along the paths of nerve contact on these cells. The changes, at individual 3–5-μm foci, reflected all the permutations possible among the separate kinds of AChR accumulation shown in Fig. 1, and can most simply be understood as either increases or decreases in the size of the AChR aggregates at the site of nerve–muscle contact. Even though virtually all of the conceivable changes occurred, the relative numbers of each transition were again different (Table II).

Thus changes from spots and clusters into the larger patches or bands (Fig. 1) were more common than the reverse. In fact, there was an obvious increase in the receptor organization at 52% of the foci shown in Table II. Changes in AChR organization were actually more common than they appear by the criteria used in Table I. Even those nerve-contacted muscle cells that remained in stage IV (Table I) consisted of approximately equal numbers of examples that either increased or decreased uniformly in AChR organization at several foci along the path of cell contact (data not shown).

Deposition of HSPG at Nerve–Muscle Contacts

In adult muscle, growing motor neurites appear to seek out specialized regions of synaptic basal lamina during synapse regeneration. In these ablation experiments, the muscle basal lamina retained polyanions (such as HSPG) stainable with ruthenium red (32). An earlier study has also reported that dense plaques of a basal lamina HSPG occur on aneural *Xenopus* embryonic muscle cells, and that some plaques are associated with adjacent AChR clusters (4). It was thus of interest to determine whether developing neurites might simply seek out these sites of basal lamina specialization during synapse formation in embryonic muscle. In order to examine this possibility, we determined the time course of HSPG accumulation during synaptogenesis in cell culture.

Nerve-free muscle cultures were exposed to TRITC-conjugated monoclonal antibody (2AC2) immediately before the addition of dissociated neural tube cells (see Materials and Methods). A low concentration of the fluorescent antibody (~100 ng/ml) was later retained in the culture medium to ensure that HSPG subsequently deposited on the cell surface

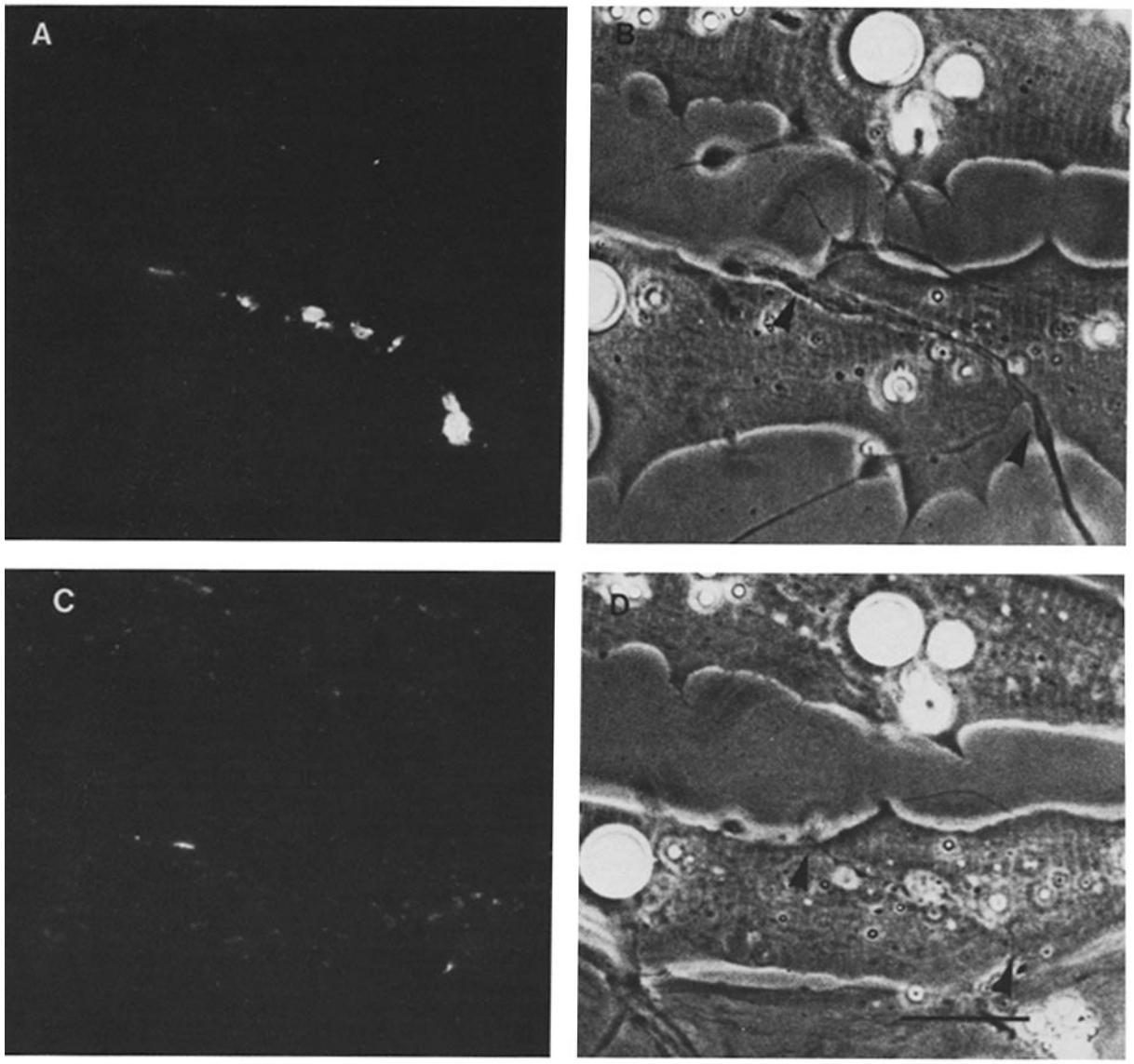

FIGURE 4 Lability of embryonic junctional AChR accumulations after denervation. Differences in AChR staining are shown between one (*A* and *B*) and two days (C and *D*) after adding dissociated nerve cells to muscle cultures that had been pulse-stained with TRITC-αBGT. Note the disappearance of AChR aggregates when part of the nerve fasicle disappeared (see arrows in *B* and *D*). Bar, 40 μm. × 600.

would also become stained. Successive observations were then made of the fluorescent staining on individual nerve-contacted muscle cells at intervals of ~24 hours (see Fig. 5).[4]

[4] These observations with fluorescent antibody provided a technical advantage not available in similar experiments (see above) with fluorescent αBGT. TRITC label associated with AChR–αBGT complexes on the muscle surface gradually became internalized over 2–3 d, eventually appearing in scattered cytoplasmic granules (data not shown). This presumably reflects the accumulation of degraded dye–toxin conjugates in secondary lysosomes (29). Such cytoplasmic stain was, in some cases, difficult to distinguish from surface AChR clusters of similar size. This restricted the period over which changes in surface AChR organization could be monitored reliably. Because analogous cytoplasmic inclusions of the stain did not become evident with TRITC-labeled antibody, it was possible to monitor changes in HSPG organization for more extended periods, often up to 5 d. These experiments were, instead, limited by either the bleaching of the fluorochrome during the preparation of fluorescence micrographs, or the lifetime of the selected cells in the small, sealed culture chambers (see Materials and Methods).

Inasmuch as clusters of junctional AChR are associated with virtually congruent accumulations of HSPG (4), it was also possible to describe different forms of junctional HSPG organization by criteria similar to those used in Figs. 1 and 2 (see Table III). The results of this experiment indicated that changes in HSPG organization were almost as common as those observed with AChR (compare Table III with Table I). The HSPG plaques that were initially present along paths of nerve–muscle contact often grew progressively between observations, and new HSPG plaques appeared where none had been detectable previously (Fig. 5). These observations demonstrate that the deposition of junctional HSPG is a gradual process that occurs after the establishment of nerve–muscle contact, and follows a time course very similar to the aggregation of junctional AChR.

Whereas junctional HSPG progressed through forms of surface organization similar to those observed for junctional AChR aggregates (compare Figs. 3 and 5), there were notable differences in the time courses of their accumulation. The

TABLE II

Changes in ACh Receptor Organization at Individual 3–5 μm Foci along the Paths of Nerve–Muscle Contact

Initial form	Total	Percentage of foci on day 2				
		Blank	Spot	Cluster	Patch	Band
	n			%		
Blank	153	—	41	21	33	5
Spot	196	38	26	12	21	3
Cluster	131	19	8	16	38	19
Patch	129	13	9	16	43	19
Band	11	18	9	9	18	46

Changes in AChR organization at separate foci (see Fig. 1) along apparently stable paths of nerve–muscle contact from 62 of the cells (stages IV–V, Fig. 2) in Table I *A*. No attempt was made to count the number of foci which had no AChR accumulations (Fig. 1), at either observation ("blank"). Note the variability in the net rate of change at different foci, and the preponderance of examples where AChR organization increased (*large print*) by the criteria in Fig. 1.

most conspicuous difference was the stability of existing extrajunctional deposits during their accumulation in the region of nerve–muscle contact. Unlike extrajunctional AChR clusters, which disappeared during synaptogenesis (2, 3), extrajunctional HSPG deposits either retained their original configuration (Fig. 5) or grew in size. Once they had formed, junctional HSPG deposits also appeared remarkably stable (compare Fig. 4 and 6). They did not show the shrinkage sometimes seen with corresponding junctional AChR clusters, (Tables I and II), and did not disappear upon loss of the original nerve contact (Fig. 6 and Table III). Revealing exceptions to this general rule did occur, and will be the subject of more extensive analysis in future reports (Anderson, M. J., manuscript in preparation). It is, nevertheless, reasonable to conclude from these observations that the appearance of the dense HSPG plaque at the developing neuromuscular junction is induced by the motor nerve, and follows a time course very similar to the clustering of junctional AChR.

Ultrastructure of Identified Nerve–Muscle Contacts

The above cytochemical experiments have shown that linked processes of AChR aggregation and HSPG deposition occur on the muscle cell surface after nerve contact. Previous observations have indicated that this change in AChR organization occurs only on functionally innervated muscle cells, where it parallels increases in the level of spontaneous synaptic activity (5, 22). This suggests that AChR accumulation, reflected in changes between the forms of AChR organization shown in Fig. 1, represents a localized postsynaptic differentiation at the developing neuromuscular junction. In ultrastructural studies of adult muscle, junctional AChR and HSPG have been found to be concentrated at sites of increased heavy-metal staining in the postsynaptic membrane (17) and the synaptic basal lamina (4), respectively. In the present study we have examined selected nerve-contacted muscle cells to determine whether the accumulation of AChR and HSPG (see above) might also reflect the development of these ultrastructural correlates. Cell culture is particularly suited for these experiments because it is possible to select individual paths of nerve–muscle contact at different stages of synapse development (see Fig. 2), and serially section the junctions transverse to the direction of nerve growth. When cells at different stages of development are examined in this manner, it is possible to compare their level of ultrastructural differentiation, and reconstruct the time course of synaptic development.

This analysis was carried out at two levels. In initial experiments muscle cells were selected that had either no AChR accumulation (stage 1, Fig. 2) or extensive bands of AChR (stage V, Fig. 2) along the path of nerve–muscle contact. These cells were sectioned, transverse to the nerve, and examined for the presence of ultrastructural differentiation. When these observations indicated that stage V cells (Fig. 2) all showed extensive evidence of synaptic ultrastructure, additional experiments were included to obtain more detailed information about the time course of synaptic differentiation.

These experiments involved serially sectioning along the entire path of nerve–muscle contact, and comparing the level of morphological differentiation in adjacent, ~2-μm segments (see Materials and Methods). The morphological differentiation along each of the selected paths of nerve–muscle contact was reconstructed by plotting the fraction of recovered sections (from each sequential grid) that contained elements of synaptic ultrastructure, as a function of grid number (see Materials and Methods). Individual sections were scored for (*a*) the presence of synaptic vesicles, (*b*) clusters of five or more synaptic vesicles, (*c*) presynaptic densities, and (*d*) organized basal lamina material in the extracellular space between the nerve fiber and muscle surface. In the latter case, dense staining of the sarcolemma (postsynaptic density) was invariably found to be co-extensive with the discrete tufts of junctional basal lamina. Examples of such serial reconstructions are shown in Fig. 7, *A–C* for representative muscle cells at stages III–V (Fig. 2). The pattern of AChR staining on the

TABLE III

Changes in Proteoglycan Organization

A. Changes in HSPG organization on identified muscle cells when nerve contacts remained intact

Initial stage	Number of cells	Percentage of cells on day 2 (stage)				
		I	II	III	IV	V
	n			%		
I	25	64	16	8	12	0
II	16	0	38	44	19	0
III	31	0	3	26	68	3
IV	39	0	0	0	87	13
V	1	0	0	0	0	100

B. Changes in HSPG organization when the nerve disappeared

Initial stage	Number of cells	Number of cells on day 2 (stage)				
		I	II	III	IV	V
I	4	4	0	0	0	0
II	1	0	0	0	1	0
III	5	0	0	1	3	1
IV	7	0	0	0	6	1

Changes in proteoglycan organization at different sites of nerve–muscle contact between 1 and 2 d after plating neural tube cells. Junctional HSPG deposits were classifed by the same criteria used (see Fig. 2) for AChR accumulations in Table I. The population of cells was again divided into separate groups where the path of nerve–muscle contact appeared to have remained intact (*A*), and where the original nerve fiber disappeared (*B*). Note the progressive increase in HSPG organization (*large print*) along most paths of nerve–muscle contact, analogous to that observed for AChR (compare with Table I), except that virtually no decreases in HSPG area were observed (*fine print*), even upon loss of the nerve.

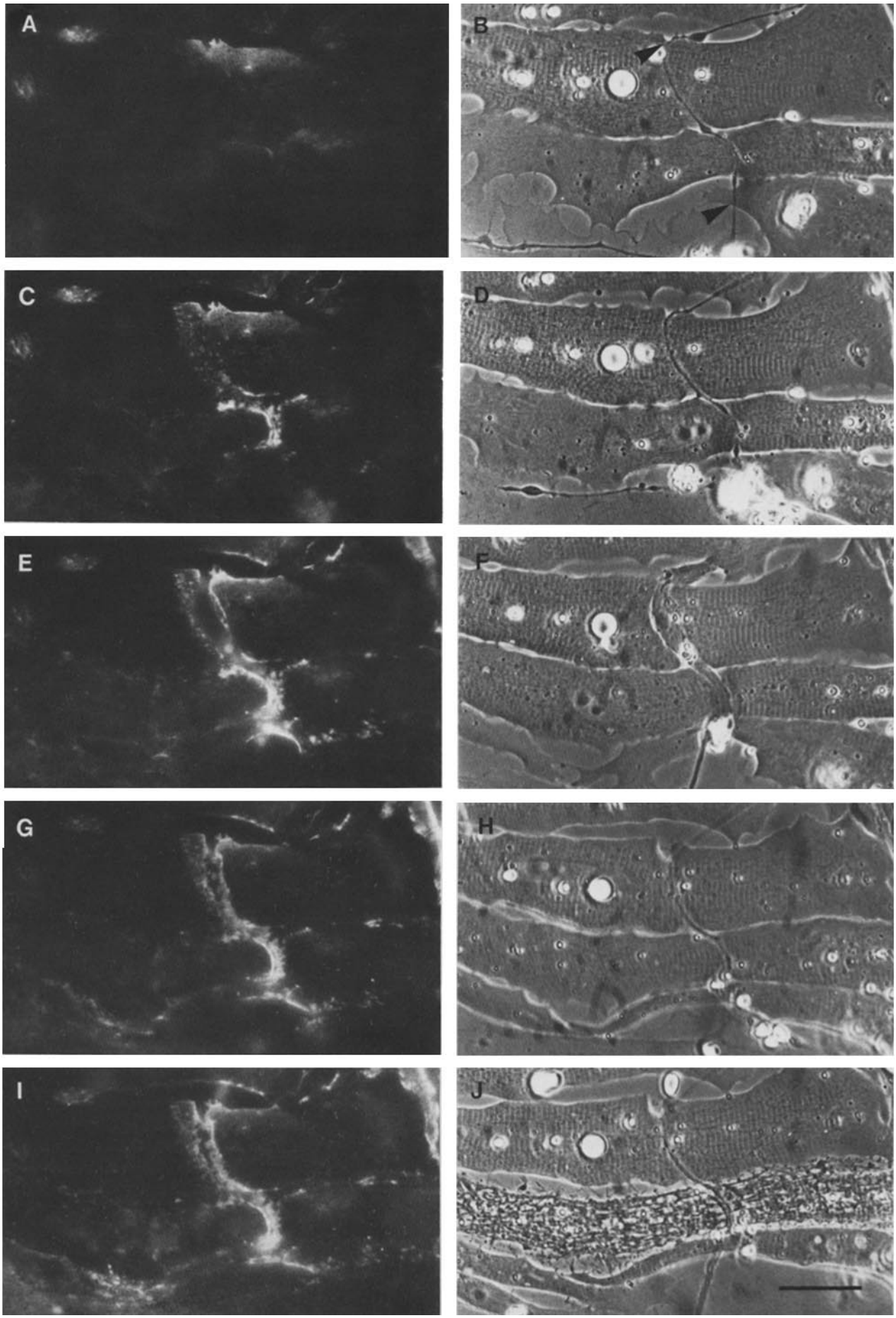

FIGURE 5 Proteoglycan organization on individual nerve-contacted (see arrows in *B*) muscle cells, after 1 (*A* and *B*), 2 (*C* and *D*), 3 (*E* and *F*), 4 (*G* and *H*), and 5 (*I* and *J*) d of nerve growth in the presence of TRITC-labeled monoclonal antibody (2AC2). There was a gradual appearance of brightly stained HSPG plaques (*A*, *C*, and *E*) along the existing path of nerve contact with two adjacent muscle cells (*B*, *D*, and *F*). The HSPG organization on each cell followed a progression equivalent to changes between stages I–V in Fig. 2. Note also the gradual fading of the fluorescent image from *A* to *I*. Bar, 40 μm. × 400.

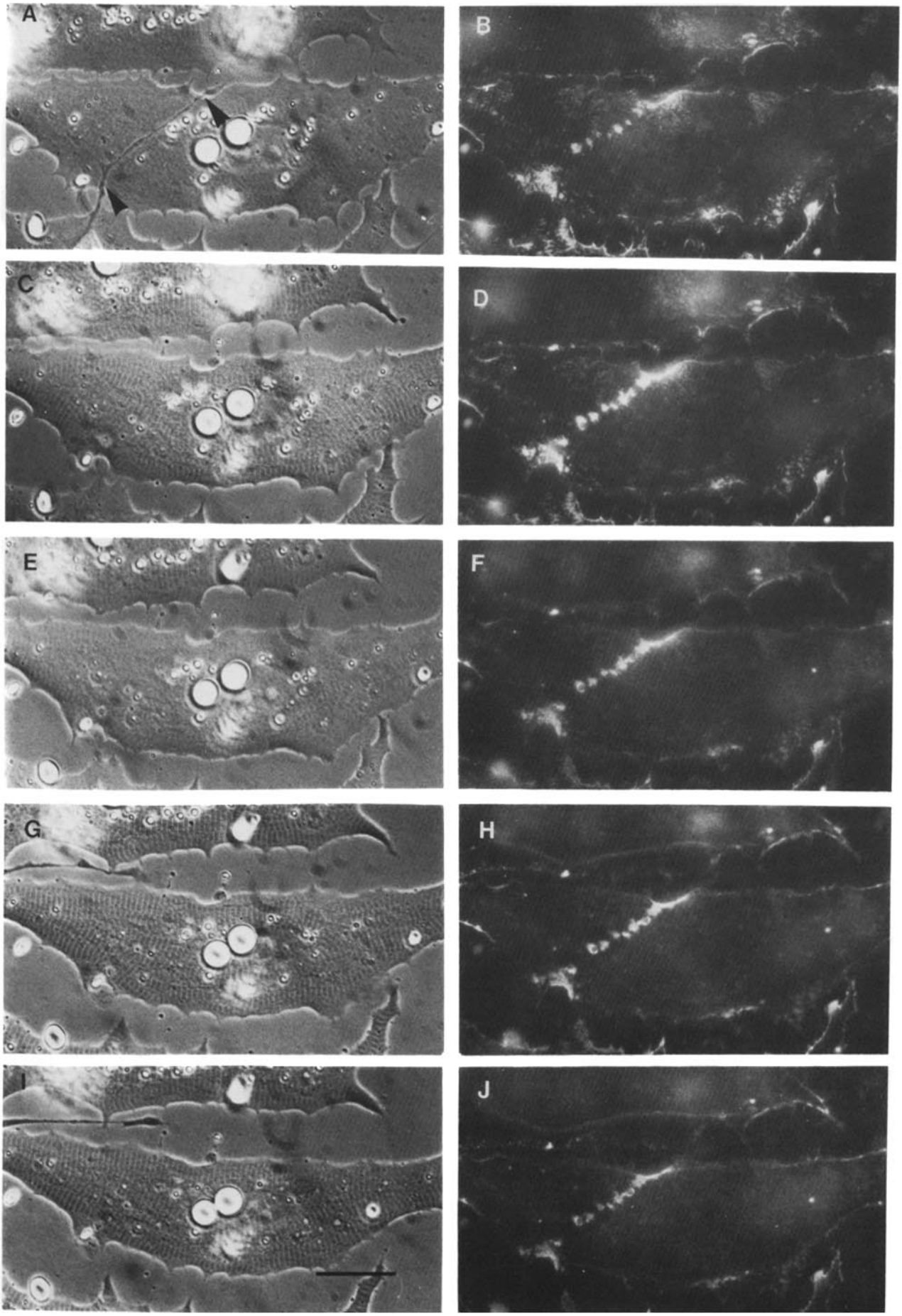

FIGURE 6 Stability of junctional proteoglycan deposits after denervation. The experimental conditions were similar to those described in Fig. 5, except that the nerve (see arrowheads in *A*) disappeared between the first (*A* and *B*). and second day (*C* and *D*) in culture. Note that HSPG organization increased at the site of nerve–muscle contact between the first and second observation (*B* and *D*) and remained static thereafter (*F*, *H*, and *J*) despite loss of the nerve (see *C*, *E*, *G*, and *I*). Note also the gradual fading of the fluorescent stain (compare *B*, *D*, *F*, *H*, and *J*) during preparation of the fluorescent micrographs. Bar, 40 μm. × 400.

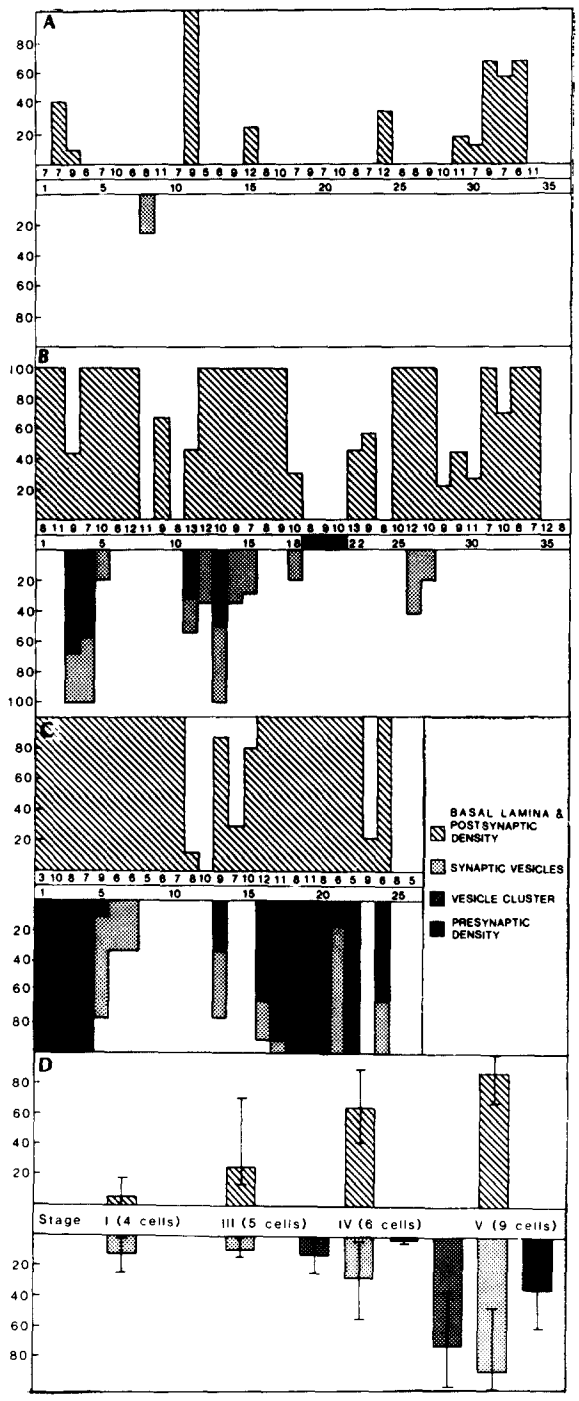

FIGURE 7 (*A–C*) Reconstruction of the ultrastructural differentiation visible along the paths of nerve–muscle contact shown in Fig. 8 (*B*, *D*, and *F*). The percentage of sections (per grid) displaying each synaptic organelle (synaptic vesicles, vesicle clusters, presynaptic densities, junctional basal lamina, and postsynaptic density) was calculated for each sequential grid (20 serial passes of the microtome knife). This value was then plotted as a function of grid number, revealing the distribution of differentiated sites along the path of cell contact. The number of recovered sections is presented above each grid number. Postsynaptic organelles are plotted in the upper panels, with the corresponding presynaptic structures beneath them. (*A*) Differentiation along the stage III contact in Fig. 8, *A* and *B*; (*B*) Along the two stage IV nerve contacts shown in Fig. 8, *C* and *D*. (*C*) Along the stage V contact in Fig. 8, *E* and *F*. (*D*) Changes in the level of ultrastructural differentiation at different stages of AChR accumulation. The percentage of recovered sections that contained each element of synaptic morphology was calculated for all cells in the sample. Average values were then calculated for the cells at each stage (Fig. 2). These values have been plotted in Fig. 7*D* as a function of stage, to reveal the developmental sequence of synaptic differentiation. The vertical bars reflect the range of values observed for the cells in each stage. Note the initial appearance of postsynaptic differentiation followed by the presynaptic appearance of vesicle clusters and then presynaptic densities opposite specialized regions on the muscle surface (see also arrow in Fig. 9*C*). Note in particular, the considerable variation in the extent of morphological differentiation at adjacent regions along the nerve at all stages (*A*, *B*, and *C*).

same cells is shown in Fig. 8. Several features of the developing neuromuscular junctions in this preparation became apparent from this analysis. For example, synaptic differentiation was commonly restricted to a few discrete regions scattered along the path of nerve–muscle contact, as was previously shown for the developing accumulations of junctional AChR and HSPG (Figs. 1–6). Likewise, when presynaptic differentiation of vesicle clusters first became detectable at stage IV (Fig. 7*B*), it was invariably located opposite organized regions of junctional basal lamina. However, organized plaques of junctional basal lamina were commonly observed without corresponding evidence of a presynaptic apparatus. This was most conspicuous at stages III and IV (Figs. 7, *A* and *B*).

To determine the sequence of developmental changes in synaptic differentiation, we computed the fraction of recovered sections containing the different synaptic organelles (see above) for each path of nerve–muscle contact. This analysis is shown in Fig. 7*D*, which compares the fraction of recovered sections containing elements of synaptic ultrastructure at the different stages of AChR accumulation illustrated in Fig. 2. The vertical bars on each column illustrate the range of variation observed between all the cells examined at each stage. Although there was significant variation in the extent of synaptic differentiation within the individual stages of AChR accumulation shown in Fig. 2, this was notably less than that found between cells at different stages.

Several conclusions can be drawn from the data compiled in Fig. 7*D*. Most significant for this study is the progressive increase, at different stages of AChR accumulation, in the proportion of the cell contact that showed a discrete, organized junctional basal lamina. Because the observations shown in Figs. 3 and 5, as well as in Tables I and III, clearly indicate that individual nerve–muscle contacts undergo time-dependent increases in stage by the criteria illustrated in Fig. 2, it is reasonable to conclude that they also undergo a corresponding development of an organized junctional basal lamina. As was the case for the deposition of junctional HSPG, the junctional basal lamina represented a localized synaptic differentiation (also illustrated by the micrographs shown in Fig. 9, *A–C*). Thus most of the extrasynaptic muscle cell surface remained devoid of an organized, ultrastructural basal lamina even at advanced stages of synaptic differentiation where basal lamina extended for almost the full length of cell contact. Taken together, these observations lead to the conclusion that the plaque of basal lamina at the neuromuscular junction is induced by nerve–muscle interaction, as are the junctional accumulations of AChR and HSPG.

The observations summarized in Fig. 7*D* also reveal significant differences in the time course of pre- and postsynaptic differentiation. Thus an extensive junctional basal lamina became detectable at stages III and IV (Fig. 2), virtually

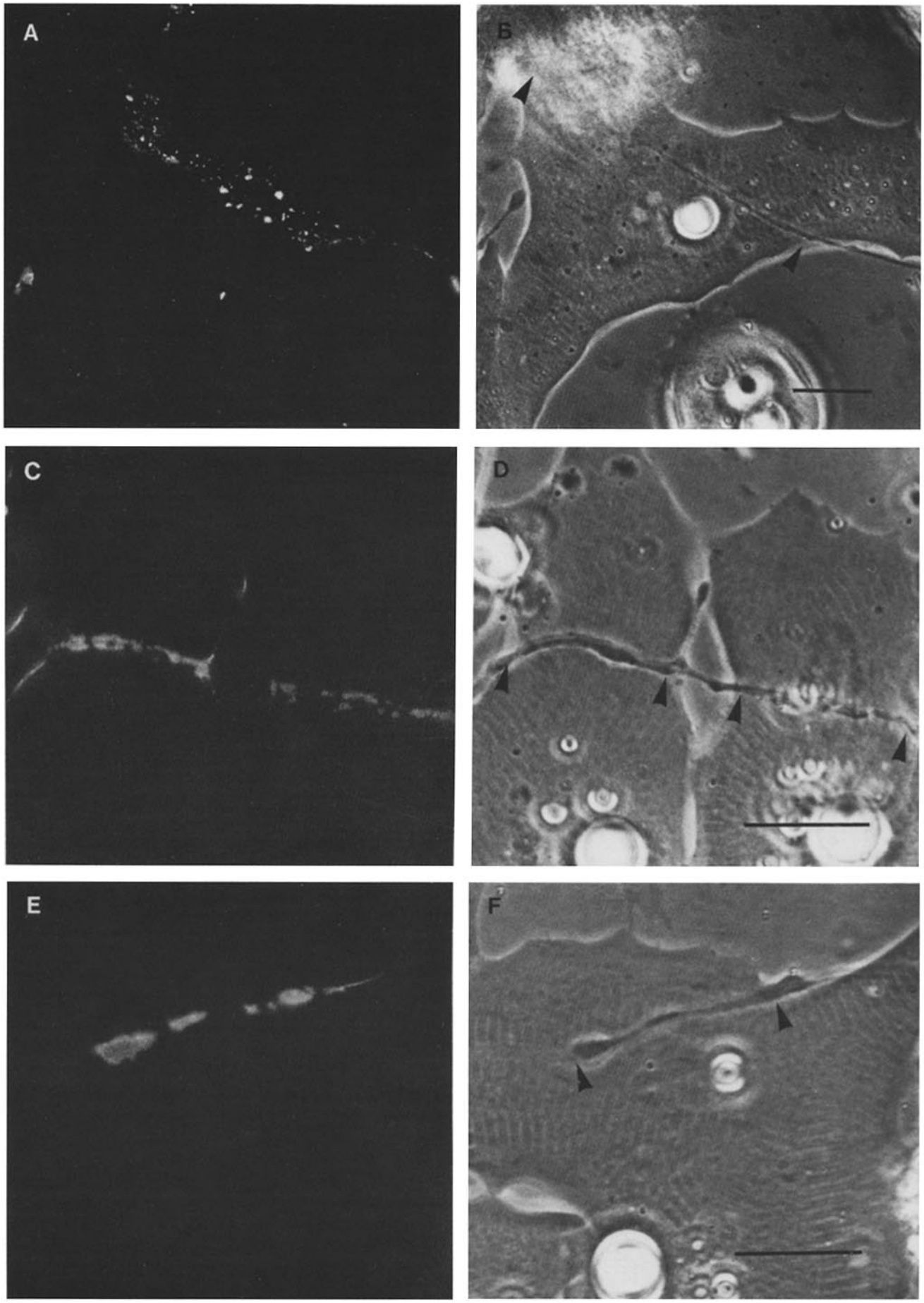

FIGURE 8 Different stages of junctional AChR organization on the individual muscle cells selected for ultrastructural analysis. The cells were serially sectioned transverse to the paths of the nerve fibers (see arrows in *B*, *D*, and *F*) after selection for AChR organization at stages III (*A*), IV (*C*), and V (*E*), by the criteria illustrated in Fig. 2. Serial reconstructions of the morphological features visible in sequential grids are presented in Fig. 7. Examples of the structural differentiation visible in the cell in *E* and *F* are shown in Fig. 9. Bars, 30 μm. (*B*) × 500. (*D* and *F*) × 800.

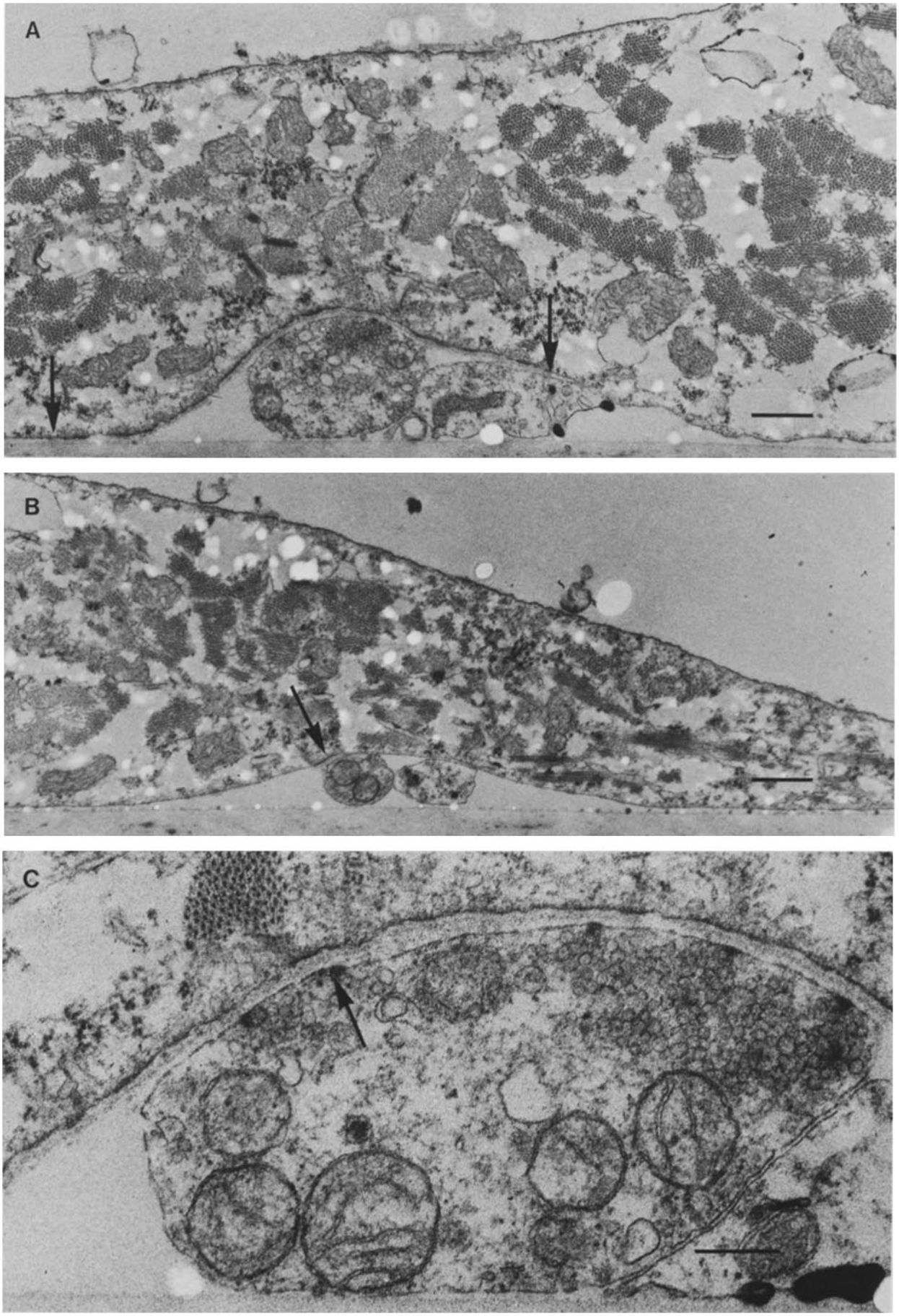
A
B
C

coincident with the corresponding accumulation of AChR and HSPG. On many of the cells at these stages, however, there was no evidence of the synaptic vesicle clusters (see also Fig. 7, *A* and *B*), which became obvious at later stages. It should be noted, nevertheless, that this apparent retardation of presynaptic differentation merely reflected a delay in the appearance of ultrastructurally detectable presynaptic organelles. Previous work in this system has already demonstrated that spontaneous, quantal transmitter release can be detected by electrophysiological methods at much earlier stages of synaptic development, even before the appearance of junctional AChR aggregates (5, 22).

DISCUSSION

In the present study we have used fluorescent toxin and antibody derivatives to examine nerve-induced changes in the organization of the muscle cell surface during development of the neuromuscular junction. Previous studies of this preparation (5, 22) have indicated that quantitative changes in the properties of spontaneous synaptic potentials also correlate with increases in the postsynaptic clustering of AChR. Our observations indicate that a coordinated process of AChR clustering and HSPG deposition occurs at discrete sites along the path of cell contact, contributing to the eventual development of a morphologically recognizable neuromuscular junction. Since these changes occurred after the establishment of nerve–muscle contact, it is reasonable to conclude that both AChR clustering and HSPG deposition are induced by the developing motor neurite.

The time courses of AChR aggregation and HSPG deposition were found to vary considerably in rate, both on different muscle cells and at adjacent sites along a single path of nerve–muscle contact. On individual muscle cells this variability ultimately led to the development of discrete regions of extensive synaptic differentiation separated by variable lengths of undifferentiated nerve–muscle contact (compare Figs. 7*C*; 8, *E* and *F*; and 9, *A* and *B*).

Interestingly, recognizable presynaptic differentiation in the nerve fiber (consisting of synaptic vesicle clusters and discrete presynaptic densities) developed late, after the formation of extensive postsynaptic specialization. This observation was unexpected since previous work (5, 22) has indicated that spontaneous, quantal transmitter release, presumably originating from synaptic vesicles, begins well before postsynaptic AChR specialization becomes evident with these methods. Transmitter release at the developing junction may either involve nonvesicular ACh, or, more likely, the synaptic vesicles present at these early stages of synaptogenesis are not well preserved by conventional fixation techniques (8).

Our observations have shown that there is a close correspondence between the localization of AChR and HSPG at developing neuromuscular junctions. These substances appear together (4) in discrete, organized accumulations scattered throughout a perineural zone, which extends laterally for several micrometers on either side of the region of cell contact. The growing aggregates eventually fuse and fill this perineural region, where they appear to be associated with an organized ultrastructural plaque of densely stained postsynaptic membrane with an associated, localized specialization of the basal lamina (see arrows, Fig. 9, *A* and *B*). As occurs in vivo (23), the developing junction at this stage is still devoid of both Schwann cell and any morphologically distinguishable, nerve-associated basal lamina (Fig. 9). From these observations, it would appear that the developing junctional basal lamina, including HSPG, behaves as if it were a postsynaptic structure induced by the nerve fiber. The results, however, do not formally exclude the possibility that the junctional basal lamina could actually contain molecules synthesized by the developing motor neuron.

Whereas there was a close correspondence between the appearance and growth of AChR clusters and their associated HSPG deposits at developing junctions, changes in the organization of these markers elsewhere on the muscle cell appeared quite different. AChR clusters away from the path of nerve contact disappeared during AChR accumulation at the developing junction (2, 3) whereas extrajunctional deposits of HSPG either remained unchanged, or continued to grow (Fig. 5). It has already been shown that this change in AChR organization reflects a rearrangement of mobile AChR units within the sarcolemma (2). Mobile AChR thus disappeared from one set of stable, specialized sites of HSPG deposition on the muscle cell, and became associated with new sites forming along the path of the nerve. Once localized along the nerve, AChR clusters still appeared relatively unstable, and commonly disappeared after denervation (Fig. 4 and Table I). In contrast, junctional HSPG deposits appeared stable and could survive both denervation (Fig. 6 and Table III) and the degeneration of the muscle cell (see Fig. 5). This indicates that the denervated embryonic end plates lost their junctional aggregates of AChR, but retained a trace of specialized basal lamina containing a high concentration of HSPG. This is consistent with the observed stability of the adult junctional basal lamina (12, 32), and may also help to explain the remarkable reappearance of junctional AChE at ectopic endplates during reinnervation at the original junctions (25, 34). Despite their conspicuous similarities in distribution (4) this difference in stability suggests that different cellular mechanisms may regulate the surface organization of AChR and HSPG. This possibility will be considered in greater detail in a future report (Anderson, M. J., manuscript in preparation).

Our observations (see also reference 4) indicate that HSPG accumulation within a specialized junctional basal lamina develops coincidentally, both spatially and temporally, with the earliest junctional AChR aggregates. These substances also show similar distributions at adult neuromuscular junctions, and even at the extrajunctional AChR aggregates that form on aneural muscle cells in culture (4). Furthermore, it has been shown that the junctional basal lamina is able to

FIGURE 9 Local variation in ultrastructural differentiation along the stage V nerve-muscle contact shown in Figs. 8, *E* and *F*, and 7*C*. As shown quantitatively in Fig. 7*C*, adjacent regions showed both extensive (*A* and C) and minimal (*B*) evidence of synaptic differentiation. Postsynaptic specialization of the sarcolemma (arrows in *A* and *B*) was invariably associated with a corresponding plaque of basal lamina (*A* and C), and commonly extended well beyond the site of cell contact (see arrows in *A*). (C) A higher magnification of the nerve in the grid adjacent to that in *A* (grid 2 in Fig. 7*C*) showing the relevant elements of synaptic structure scored for the analyses in Fig. 7: postsynaptic density adjacent to the basal lamina, and clusters of synaptic vesicles around discrete presynaptic densities (arrow). Note that most of the muscle surface was devoid of basal lamina. Bars: (*A* and *B*) 1 μm; (C) 0.5 μm. (*A* and *B*) × 15,000. (C) × 41,000.

induce AChR aggregation in regenerating adult muscle fibers (12). Taken together, these observations suggest that the clustering of junctional AChR is secondary to a nerve-induced deposition of a junctional basal lamina. Unlike adult junctional AChR aggregates, however, those present at the developing neuromuscular junction (33), or on aneural muscle cells (2, 3, 10), appear to be unstable. The maintenance of AChR clusters on embryonic muscle cells thus requires more than the presence of a specialized basal lamina, and appears also to be dependent upon some ongoing process in the muscle cell that requires ATP (10). In fact, the association between AChR and HSPG may be indirect, reflecting an interaction between AChR and a transmembrane complex composed of several structural proteins (4, 11, 18, 20). It remains unclear how the motor nerve causes AChR to dissociate from extrajunctional sites containing HSPG while aggregating at similar sites developing along the path of nerve–muscle contact.

The experiments described in this report have shown that motor neurites induce the appearance of a high concentration of HSPG associated with the developing junctional basal lamina. Synaptogenesis in embryonic muscle thus differs from that which occurs during the reinnervation of denervated adult muscle, where growing neurites appear to seek out existing specializations of the basal lamina (32). However, it is worth noting that the preference of regenerating nerve for existing differentiated sites on adult skeletal muscle may not be absolute, in that ectopic neuromuscular junctions can form under some experimental conditions (19, 24). Instead, it would seem either that embryonic nerves are more proficient at inducing the deposition of a junctional basal lamina, or that the embryonic muscle is more receptive to the inductive action of the nerve. This difference may be related to the fact that adult, but not embryonic muscle, is surrounded by a sheath composed of basal lamina and other elements of extracellular matrix (21). This extracellular matrix could conceivably shield the adult muscle fiber from the inductive action of the nerve, or block processes of cell recognition which may be necessary for the initiation of synaptic differentiation.

In another respect, however, our observations do appear consistent with the phenomenology of synapse regeneration. It has been shown that presynaptic differentiation within regenerating motor nerve terminals (32), and the accumulation of "junctional" AChR aggregates (12) can both be induced by elements of the junctional basal lamina. Our results indicate that clusters of synaptic vesicles and the developing aggregates of junctional AChR preferentially form opposite regions of postsynaptic differentiation, which include a junctional accumulation of basal lamina HSPG. This observation suggests that the formation of a specialized junctional basal lamina, induced by the nerve, may in turn stimulate further localized differentiation in both the muscle and the neurite. If this should be the case, it would insure that sites of transmitter release become spatially matched with appropriate regions of chemosensitive postsynaptic membrane.

We are grateful to Dr. M. Hollenberg, Dr. K. Muller, Dr. D. Schubert, and Dr. J. Steinback for their valuable comments on the manuscript, and to Dr. D. M. Fambrough and Dr. S. Heinemann for many useful suggestions. We are indebted to Ms. Caroline Collins for the preparation of the manuscript.

This work was supported by grants from the Muscular Dystrophy Association of America and the National Institutes of Health (U. S. Public Health Service) to D. M. Fambrough (Carnegie Institution of Washington, Baltimore, MD) and S. H. Heinemann, (Salk Institute, LaJolla, CA) and from the Alberta Heritage Foundation for Medical Research to M. J. Anderson.

Received for publication 12 March 1984, and in revised form 9 July 1984.

REFERENCES

1. Anderson, M. J., and M. W. Cohen. 1974. Fluorescent staining of acetylcholine receptors in vertebrate skeletal muscle. *J. Physiol. (Lond.).* 237:385–400.
2. Anderson, M. J., and M. W. Cohen. 1977. Nerve-induced and spontaneous redistribution of acetylcholine receptors on cultured muscle cells. *J. Physiol. (Lond.).* 268:757–773.
3. Anderson, M. J., M. W. Cohen, and E. Zorychta. 1977. Effects of innervation on the distribution of acetylcholine receptors on cultured amphibian muscle cells. *J. Physiol. (Lond.).* 268:731–756.
4. Anderson, M. J., and D. M. Fambrough. 1983. Aggregates of acetylcholine receptors are associated with plaques of a basal lamina heparan sulfate proteoglycan on the surface of skeletal muscle fibers. *J. Cell Biol.* 97:1396–1411.
5. Anderson, M. J., Y. Kidokoro, and R. Gruener. 1979. Correlation between acetylcholine receptor localization and spontaneous synaptic potentials in cultures of nerve and muscle. *Brain. Res.* 166:185–190.
6. Axelrod, D., P. Ravdin, D. E. Koppel, J. Schlessinger, W. W. Webb, E. L. Elson, and T. R. Podleski. 1976. Lateral motion of fluorescently labeled acetylcholine receptors in membranes of developing muscle fibers. *Proc. Natl. Acad. Sci. USA.* 73:4594–4598.
7. Barker, D., and M. C. Ip. 1966. Sprouting and degeneration of mammalian motor axons in normal and de-afferentated skeletal muscle. *Proc. R. Soc. Lond. B. Biol. Sci.* 163:538–554.
8. Birks, R. I. 1974. The relationship of transmitter release and storage to fine structure in a sympathetic ganglion. *J. Neurocytol.* 3:133–160.
9. Birks, R., H. E. Huxley, and B. Katz. 1960. The fine structure of the neuromuscular junction of the frog. *J. Physiol. (Lond.).* 150:134–144.
10. Block, R. J. 1979. Dispersal and reformation of acetylcholine receptor clusters on cultured rat myotubes treated with inhibitors of energy metabolism. *J. Cell Biol.* 82:626–643.
11. Burden, S. 1982. Identification of an intracellular postsynaptic antigen at the frog neuromuscular junction. *J. Cell Biol.* 94:521–530.
12. Burden, S. J., P. B. Sargent, and U. J. McMahan. 1979. Acetylcholine receptors in regenerating muscle accumulate at original synaptic sites in the absence of nerve. *J. Cell Biol.* 82:412–425.
13. Cohen, M. W., and P. R. Weldon. 1980. Localization of acetylcholine receptors and synaptic ultrastructure at nerve-muscle contacts in culture: dependence on nerve type. *J. Cell Biol.* 86:388–401.
14. Couteaux, R. 1955. Localization of cholinesterases at neuromuscular junctions. *Int. Rev. Cytol.* 4:335–375.
15. Couteaux, R., and M. Pecot-Dechavassine. 1970. Vesicules synaptiques et poches au niveau des "zones actives" de la jonction neuromusculaire. *C. R. Hebd. Séances Acad. Sci. D.* 271:2346–2349.
16. Fambrough, D. M., A. G. Engel, and T. L. Rosenberry. 1982. Acetylcholinesterase of human erythrocytes and neuromuscular junctions: homologies revealed by monoclonal antibodies. *Proc. Natl. Acad. Sci. USA.* 79:1078–1082.
17. Fertuck, H. C., and M. M. Salpeter. 1976. Quantitation of junctional acetylcholine receptors by electron microscope autoradiography after ^{125}Iα-bungarotoxin binding at mouse neuromuscular junctions. *J. Cell Biol.* 69:144–158.
18. Froehner, S. C., V. Gulbrandsen, C. Hyman, A. Y. Yeng, R. R. Neubig, and J. B. Cohen. 1981. Immunofluorescence localization at the mammalian neuromuscular junction of the Mr 43,000 protein of *Torpedo* synaptic membranes. *Proc. Natl. Acad. Sci. USA.* 78:5230–5234.
19. Gutman, E., and J. Z. Young. 1944. The reinnervation of muscle after various periods of atrophy. *J. Anat.* 78:15–43.
20. Hall, Z. W., B. W. Lubit, and J. H. Schwartz. 1981. Cytoplasmic actin in postsynaptic structures at the neuromuscular junction. *J. Cell Biol.* 90:789–792.
21. Jacob, M., and T. L. Lentz. 1979. Localization of acetylcholine receptors by means of horseradish peroxidase-α-bungarotoxin during formation and development of the neuromuscular junction in the chick embryo. *J. Cell Biol.* 82:195–211.
22. Kidokoro, Y., M. J. Anderson, and R. Gruener. 1980. Changes in synaptic potential properties during acetylcholine receptor accumulation and neurospecific interactions in Xenopus nerve-muscle cell culture. *Dev. Biol.* 78:464–483.
23. Kullberg, R. W., T. L. Lentz, and M. W. Cohen. 1977. Development of the myotomal neuromuscular junction in *Xenopus laevis*: an electrophysiological and fine-structural study. *Dev. Biol.* 60:101–129.
24. Lømo, T., S. Pockett, and H. Sommerschild. 1981. Changes in number and distribution of synapses during ectopic synapse formation in adult rat soleus muscles. *Neurosci. Lett. Suppl.* 7:S302. (Abstr.)
25. Lømo, T., and C. R. Slater. 1980. Control of junctional acetylcholinesterase by neural and muscular influences in the rat. *J. Physiol. (Lond.).* 303:191–202.
26. McMahan, U. J., J. R. Sanes, and L. M. Marshall. 1978. Cholinesterase is associated with the basal lamina at the neuromuscular junction. *Nature (Lond.).* 193:281–282.
27. Nieuwkoop, P. D., and J. Faber. 1956. Normal table of *Xenopus laevis*. Elsevier/North Holland, Amsterdam. 2nd ed. 162–188.
28. Nudell, B. M., and A. D. Grinnell. 1982. Inverse relationship between transmitter release and terminal length in synapses on frog muscle fibers of uniform input resistance. *J. Neurosci.* 2:216–224.
29. Pumplin, D. W., and D. M. Fambrough. 1982. Turnover of acetylcholine receptors in skeletal muscle. *Annu. Rev. Physiol.* 44:319–335.
30. Ravdin, P., and D. Axelrod. 1977. Fluorescent tetramethylrhodamine derivatives of α-bungarotoxin: preparation, separation and characterization. *Anal. Biochem.* 80:585–592.
31. Sanes, J. R., and Z. W. Hall. 1979. Antibodies that bind specifically to synaptic sites on muscle fiber basal lamina. *J. Cell Biol.* 83:357–370.
32. Sanes, J. R., L. M. Marshall, and U. J. McMahan. 1978. Reinnervation of muscle fiber basal lamina after removal of myofibers. Differentiation of regenerating axons at original synaptic sites. *J. Cell Biol.* 78:176–198.
33. Slater, C. R. 1982. Neural influence on the postnatal changes in acetylcholine receptor distribution at nerve-muscle junctions in the mouse. *Dev. Biol.* 94:23–30.
34. Weinberg, C. B., and Z. W. Hall. 1979. Junctional forms of acetylcholinesterase restored at nerve-free endplates. *Dev. Biol.* 68:631–635.
35. Weldon, P. R., and M. W. Cohen. 1979. Development of synaptic ultrastructure at neuromuscular contacts in an amphibian cell culture system. *J. Neurocytol.* 8:239–259.